**Supplemental Material:**

# Radiocarbon dating informs tree fern population dynamics and disturbance history of temperate forests in south-east Australia

Melissa Fedrigo, Stephen B. Stewart, Sabine Kasel, Vladimir Levchenko, Raphael Trouvé, Craig R. Nitschke†

† Corresponding author: School of Ecosystem and Forest Sciences, University of Melbourne, 500 Yarra Blvd, Richmond, Victoria 3121, Australia. Email: craign@unimelb.edu.au; Tel: +61 3 9035 6855.

## Appendix 1: Study Area

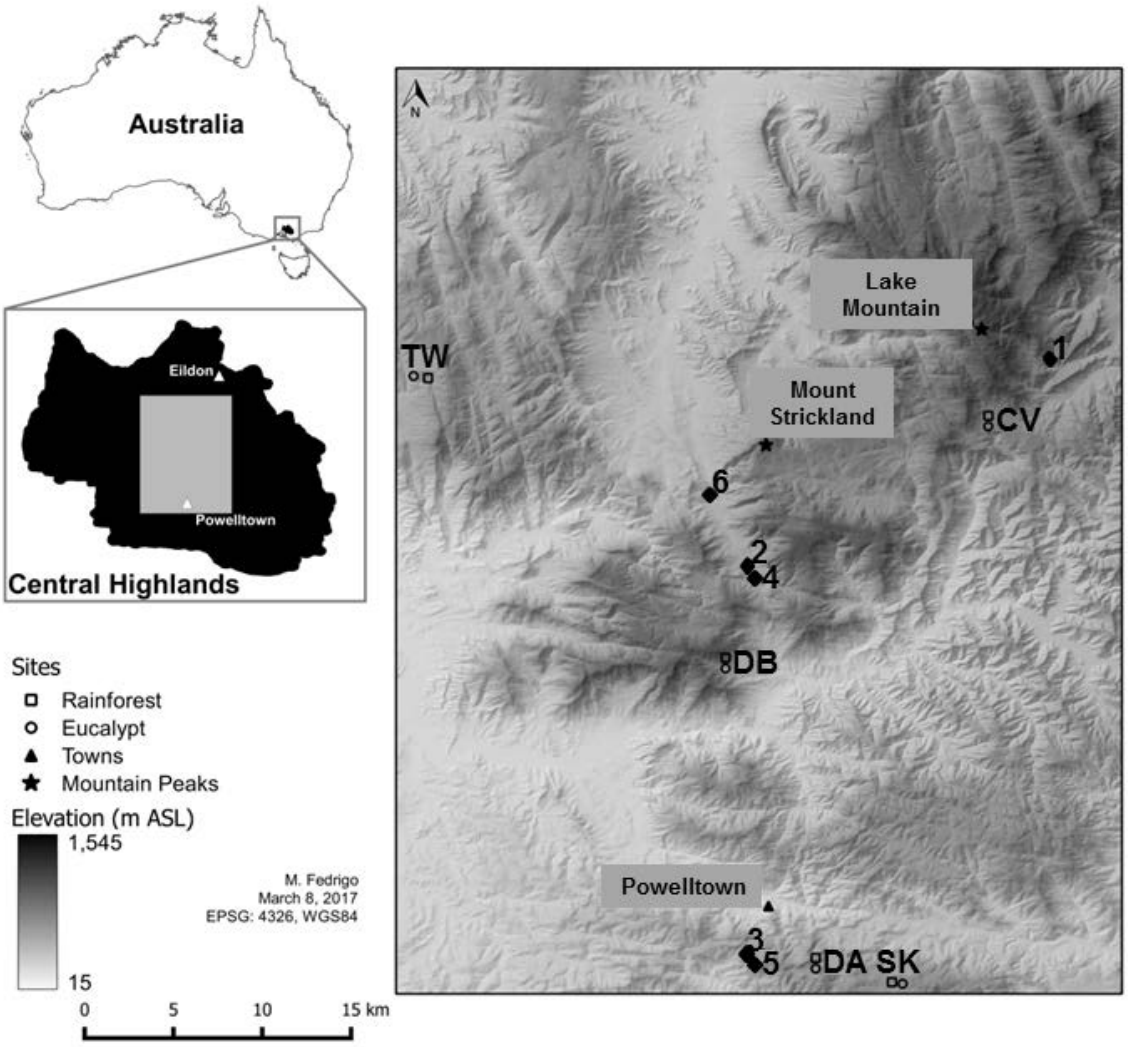


**Figure S1. Site map of the Central Highlands region showing the locations of the paired rainforest and eucalypt sites demarcated by letters (separated by less than 1 km) and tree fern harvest locations demarcated by numbers.**

**Appendix 2: Tree Ferns in cross section**

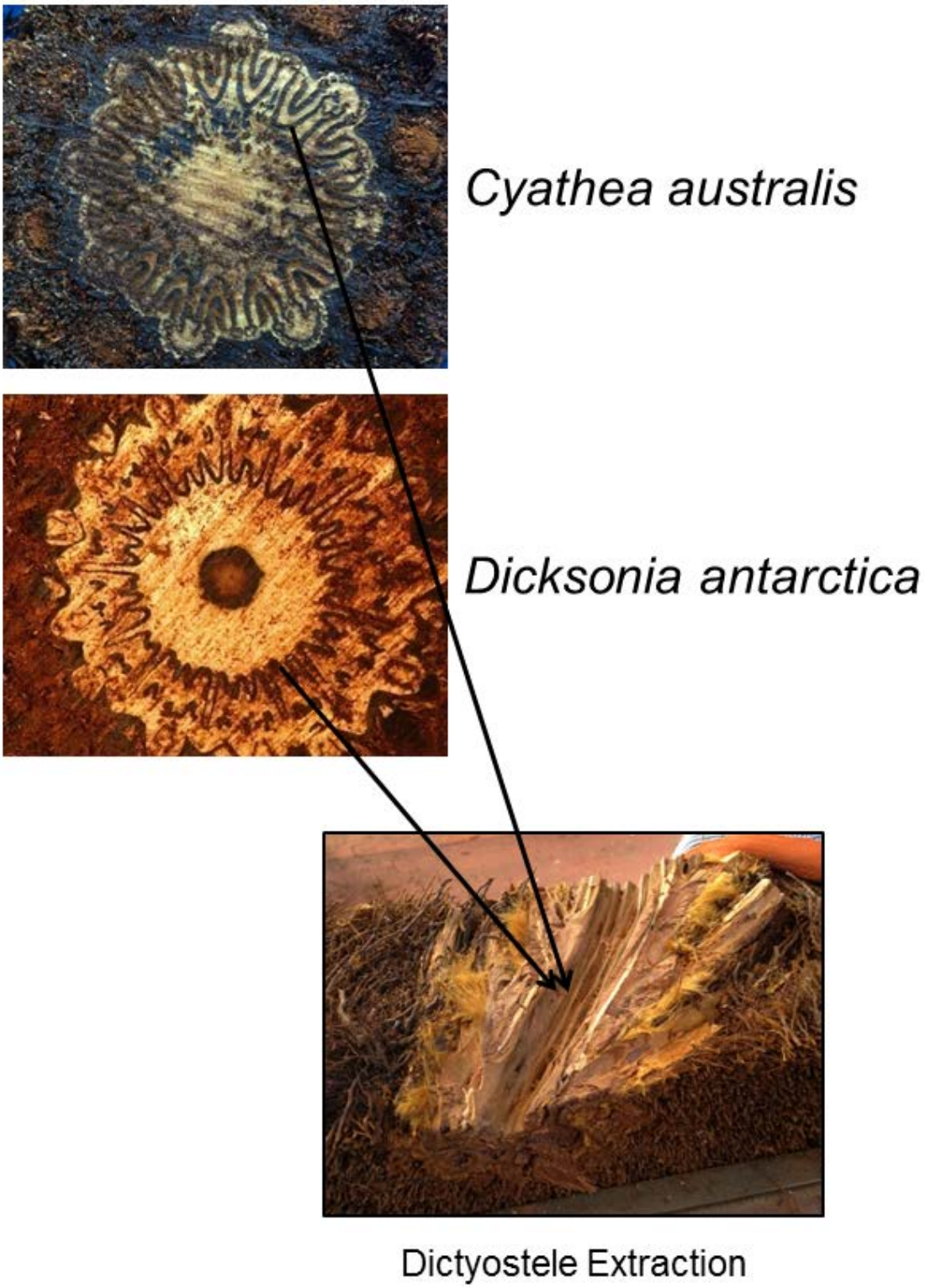


**Figure S2: Tree Ferns in cross section highlighting absence of grow rings and fibrous nature of caudex. Dark wavy lines indicated by the arrows in each cross section highlight the dictyostele where material was extracted for radiocarbon dating**

**Appendix 3**: Height-age relationships for *Cyathea australis* and *Dicksonia antarctica*. Models that performed the best according to AIC values and how close the curve reached the plot origin (0, 0).

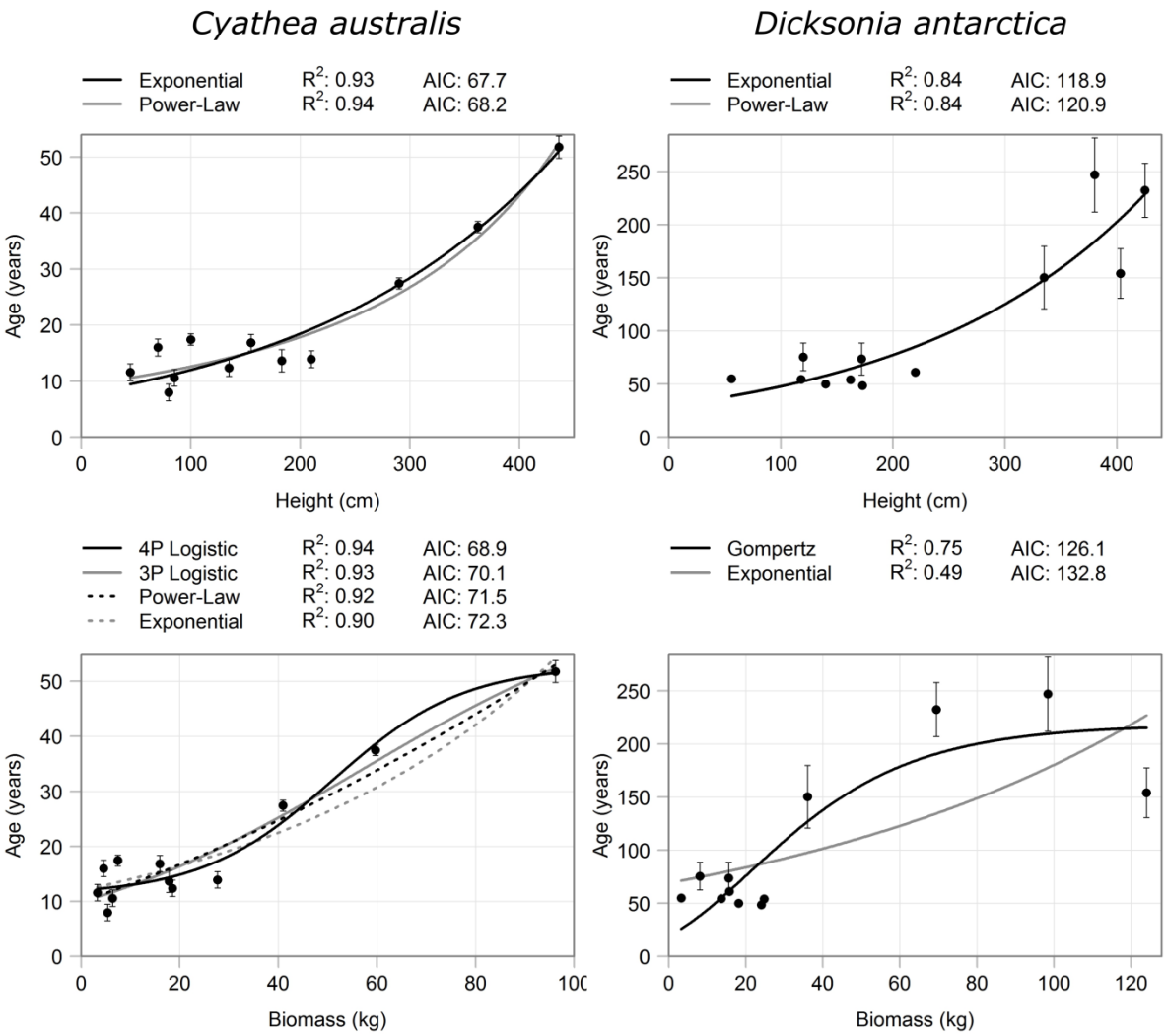


**Figure S3.** Tree fern age trajectories predicted by non-linear models (exponential, power-law, 4P logistic, 3P logistic, Gompertz) based on height and biomass for both *Cyathea australis* (left) and *Dicksonia antarctica* (right). Note, the power-law function is hidden by the exponential function in *Dicksonia antarctica*.

**Equations for tree fern age models presented in Figure S1. Bold equations are those that performed the best according to AIC values and how close the curve reached the plot origin (0, 0).**

***Cyathea australis***

**Exponential: Age ~ Height**

$$\boldsymbol{Age_{C.australis} = 7.8139372\, e^{0.0043036 \times height}}$$

AIC: 67.7

Power-Law: Age ~ Height

$$Age_{C.australis} = \left(9.27026^{1-1.385366} + 0.00123 \times height(1 - 1.385366)\right)^{\frac{1}{1-1.385366}}$$

AIC: 68.2

**4P Logistic: Age ~ Biomass**

$$\boldsymbol{Age_{C.australis} = \frac{52.842 - 11.177}{1 + e\left(\frac{50.974 - biomass}{13.284}\right)}}$$

AIC:68.9

3P Logistic: Age ~ Biomass

$$Age_{C.australis} = \frac{67.841}{1 + e\left(\frac{56.888 - biomass}{32.224}\right)}$$

AIC:70.1

Power-Law: Age ~ Biomass

$$Age_{C.australis} = \left(9.9446^{1-0.3756} + 0.1287 \times biomass(1 - 0.3756)\right)^{\frac{1}{1-0.3756}}$$

AIC: 71.5

Exponential: Age ~ Biomass

$$Age_{C.australis} = 12.015517\, e^{0.015673 \times biomass}$$

AIC: 72.3

***Dicksonia Antarctica***

**Exponential: Age ~ Height**

$\boldsymbol{Age_{D.antarctica} = 29.57e^{0.004814 \times height}}$

AIC: 118.9

Power-Law: Age ~ Height

$Age_{D.antarctica} = \left(30.054254^{1-1.020597} + 0.004364 \times height(1 - 1.020597)\right)^{\frac{1}{1-1.020597}}$

AIC:120.9

**Gompertz: Age ~ Biomass**

$\boldsymbol{Age_{D.antarctica} = 218.43224 \times e\left(-2.43256 \times 0.95923^{biomass}\right)}$

AIC: 126.1

Exponential: Age ~ Biomass

$Age_{D.antarctica} = 69.27996\, e^{0.00957 \times biomass}$

AIC: 132.8

## Appendix 4: Tree fern height distributions

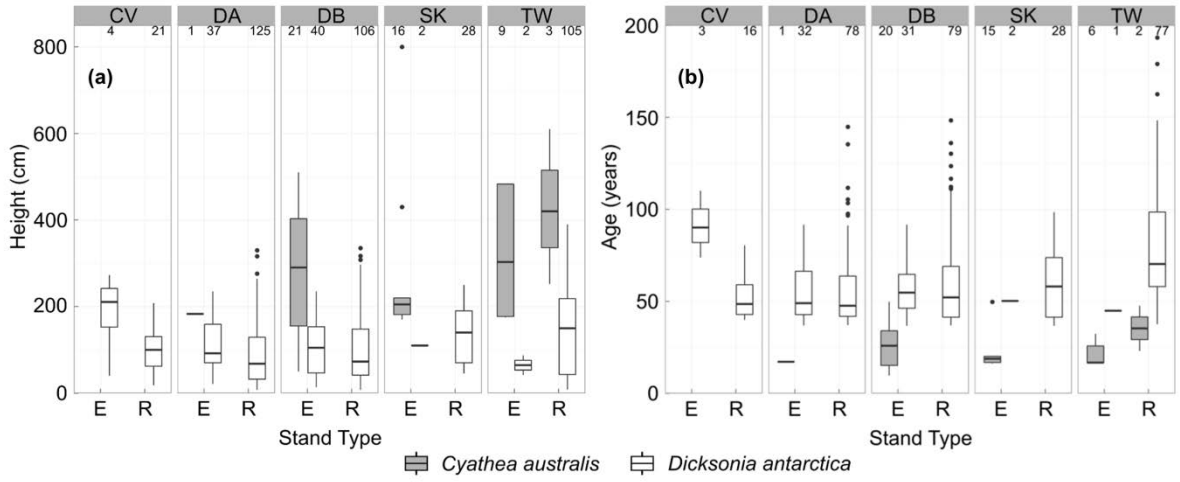


**Figure S4.** Boxplot comparison of tree fern height distributions (a) and of tree fern age distributions as predicted from height using the exponential model (b) for both *Cyathea australis* and *Dicksonia antarctica* as measured in the field in five paired Eucalypt (E) and Rainforest (R) sites. Numbers running along the top of the charts indicate *n* for each species in every site. For (b) a total of 123 *D. antactica* were excluded as height fell below the model range (<0.56 m height or <30 years in age). A total of 6 *C. australis* were excluded as height fell above the model range (>4.46 m or >51 years in age).

## Appendix 5: Tree Species-specific Dynamics

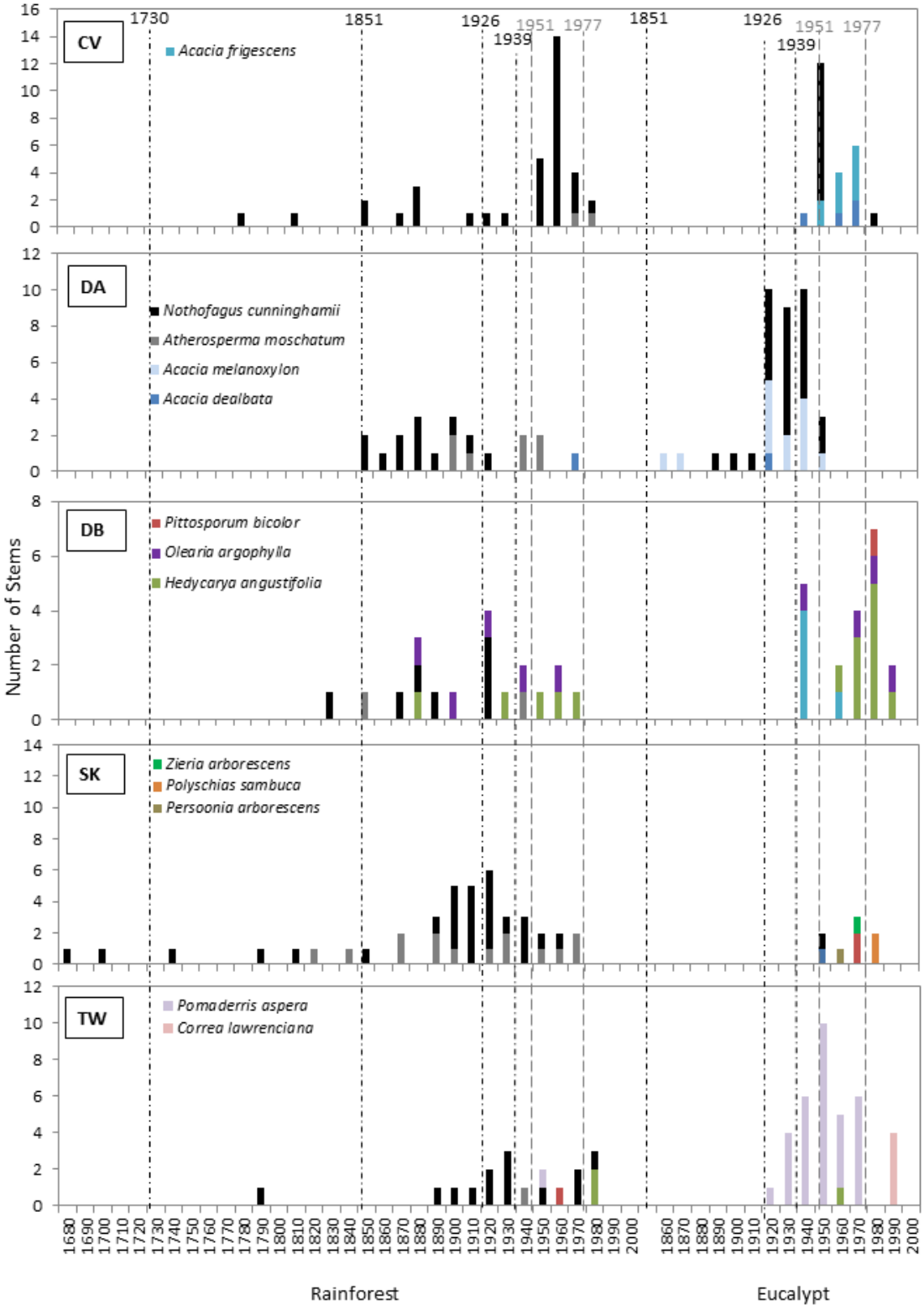


**Figure S5**. Histogram of species-specific tree ages from tree coring for paired rainforest and eucalypt sites. Establishment date indicates the year the trees reached the sampling height of 1.3 m. Dashed lines denote wildfire events (1730, 1851, 1926, 1939) reported in study area and 1951 and 1977 extreme snowfall events. Only the 1939 fire is mapped spatially for the region. The x-axis indicates the starting year for each 10 year interval.

## Appendix 6: Influence of Light on Tree Fern Age

### Methods

Leaf area index (LAI, the single-sided leaf area per unit ground area) and light available from total gap fraction in the canopy was estimated using hemispherical photography. Three to four images per fern were captured during uniform overcast conditions using a Nikon D700 camera with a Nikkon 8 mm fisheye lens. All images were analysed using the Hemisfer Light Analyser software (Hemisfer 2.2, Schleppi et al. 2007; Thimonier et al. 2010).

Linear, Power and Exponential models were used to explore the relationship between LAI and light available from total gap fraction. All analyses were done in R, version 3.3.0 (R Core Team 2016). Akaike information criterion (AIC) score were used to identify the best performing model.

### Results

Linear, Power and Exponential models for both LAI and light available from total gap fraction (LATGF) all yielded AIC values within 1.5 of each other indicating equal performance for each species X model type. Following the law of parsimony, the simplest model was chosen which in this case was the linear model. Linear models predicting tree fern age from LAI and LATGF for both species were found not be significant ($P > 0.05$) (see Fig S6). Models for *Cyathea australis* were weakly significant at $P < 0.10$ suggesting that older individuals tend be found in areas with lower LAI and higher LATGF. The uncertainty in model estimates (Fig S6) however highlight that for both tree fern species a range of tree fern ages can be found within the same LAI and a range of LAIs are associated with tree ferns of similar ages (Fig S6). These results suggest that light environment at the time of measurement is not having a confounding effect on the age–height model developed in this study.

### References

R Core Team. 2016. R: A language and environment for statistical computing. R Foundation for Statistical Computing, Vienna, Austria. https://www.R-project.org/.

Schleppi P, Conedera M, Sedivy I, Thimonier A. 2007. Correcting non-linearity and slope effects in the estimation of the leaf area index of forests from hemispherical photographs. *Agricultural and Forest Meteorology* 144: 236–242.

Thimonier A, Sedivy I, Schleppi P. 2010. Estimating leaf area index in different types of mature forest stands in Switzerland: a comparison of methods. *European Journal of Forest Research* 129: 543–562.

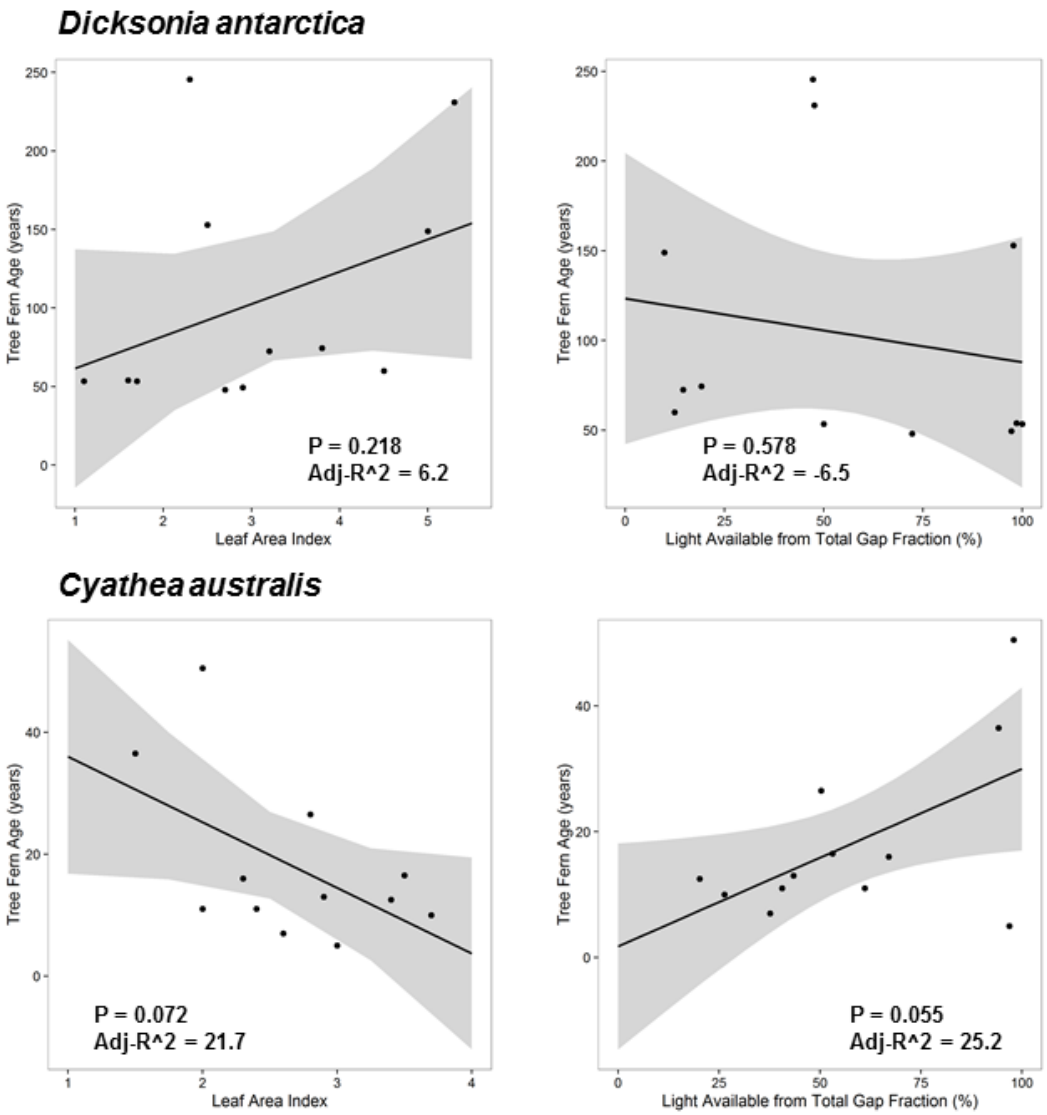


**Figure S6: Relationships between tree fern age and leaf area index (LAI) and available light. Model fit is illustrated by black line and grey ribbon (model uncertainty). All models were not significant at P = 0.05 highlighting that LAI and available light are not suitable predictors for tree fern age. For both tree fern species, a range of tree fern ages can be found within the same LAI and available light; likewise, a range of LAIs and available light % are associated with tree ferns of similar ages.**

## Appendix 7: Estimated Age Cohorts for *Eucalyptus regnans*

### Methods

To estimate the age cohorts of *Eucalyptus regnans* in each of the five sets of paired sites we calculated the potential age for each measured tree using the age-diameter model of Ashton (1976):

$$Age = DBH/1.02 \quad \textbf{(Equation 1);}$$

where Age is in years and diameter at breast height (DBH) is in cm.

The modelled tree age based on DBH proposed by Ashton (1976) could not be used to determine ages of individual trees as significant variability between diameter and stand age exists as even-aged stands of *E. regnans* can exhibit both, positive or negative skewness, or bimodal distributions (Ashton 1976). Ashton (1976) cautioned against inferring stand age from stand diameter distributions. To address this issue, we recovered the uncertainty around the age estimations from DBH by using histograms from Ashton (1976). Trees with the same diameter that occurred in stands of different ages were assigned a range of possible ages from which 95% confidence intervals were calculated. We then developed a model to estimate the uncertainty of tree age based on DBH (equation 2). We used non-linear regression in R, version 3.3.0 (R Core Team 2016) to fit the following Mitscherlich Equation (Sorensen 1983):

$$CI_{95\%}\ Age = 75 * [1-e^{(-0.009179*DBH)}] \quad \textbf{(Equation2);}$$

where Age is in years and diameter at breast height (DBH) is in cm.

The model variant with significant parameters ($P < 0.05$) and the best fit, based on AIC, were selected (see Equation 2, Fig S7).

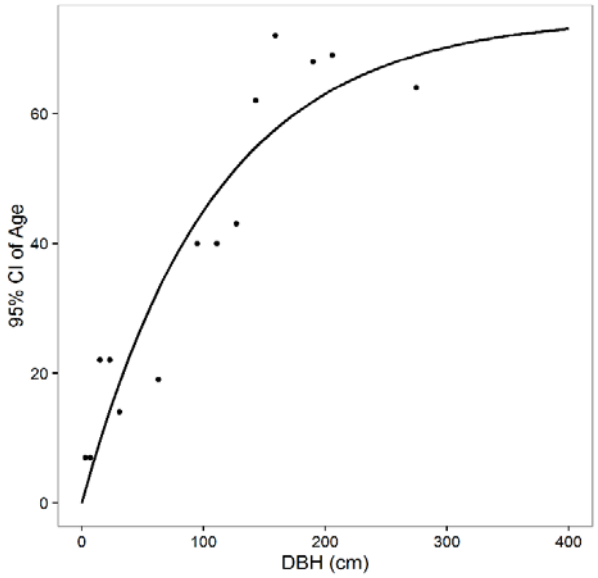


**Figure S7: Mitscherlich equation estimating the relationship between DBH of *E. regnans* and the uncertainty in age based on diameter and stand age from Ashton (1976).**

Ashton (1976) identified that even-aged *E. regnans* stands have diameter distributions that have a strong tendency to conform to a normal distribution; however, multi-aged stands can have a bimodal distribution. Stands with bimodal distributions contain populations of individuals that could be divided into subgroups, or this instance cohorts that may have recruited at different times. Model-based clustering using finite mixture models is one method that can identify subgroups within populations and assign individuals to subgroups (Benaglia et al. 2009). We used the mixtools package (Benaglia et al. 2009) in R, version 3.3.0 (R Core Team 2016), to identify the occurrence of subgroups of *E. regnans* with each plot and determine the average DBH and age of these subgroups. We used both standard normal-mixture method and semiparametric approaches (Hunter et al .2007, Benaglia et al. 2009) to identify the number of eucalypt cohorts in each plot. The final model chosen was based on the number of subgroups that maximised the log likelihood (Benaglia et al. 2009). We reclassified subgroups as age cohorts and then using the uncertainty in ages based on DBH identified in Equation 2 calculated the 95% confidence interval of age for each cohort (see Fig S8).

## Results

All eucalypt sites had multiple eucalypt cohorts with TW and DB having two, SK and CV three and DA four. Cohorts ranged from 45 to 343 years old (see Figure S8). Eucalypt cohorts at the TW eucalypt site dated to 1739 (± 69 years) and 1920 (± 43 years) which align

with the 1730 and 1926 fires, the latter signal was reflected in the understorey tree age data. The SK site had cohorts dating back to 1740 (± 68years), 1820 (± 62 years) and 1970 (± 25 years) indicating a general alignment with the 1730 and 1983 fires but not the 1851 fire in the region. Eucalypt cohorts in the DB eucalypt plots were from 1820 (± 62 years) and 1910 (± 46 years). These dates align with 1830 and 1926 *Nothofagus cunninghamii* cohorts in the rainforest site (see Figure S4). Eucalypt cohorts at the CV eucalypt site date to 1787 (± 65 years), 1836 (± 60 years) and 1966 (± 27 years). The 1836 cohort is likely from the 1851 fire and the 1944 from the 1939 fire which are evident in the rainforest tree age data (see Fig S4 and S7). Four eucalypt cohorts were identified at the DA eucalypt site, the oldest of which dated to 1672 (± 71 years). The remaining three cohorts date to 1784 (± 66 years), 1860 (± 56 years) and 1963 (± 28 years). The 1860 cohort aligns with the 1851 fire signal detected in the understorey trees while the 1963 cohort may have come from the 1926 fire that is evident in the tree core data for the plot. The 1672, 1784 and 1820 cohorts do not align with any previously recorded fires for the region. Interestingly there were multiple occurrences of strong and extended periods of summer drought in the region at these times (Palmer et al. 2015) which suggests that conditions were climatically suitable for wildfires when these cohorts potentially established.

Rainforest sites had one to two eucalypt cohorts with TW and SK having one and CV, DA and DB two. Cohorts ranged from 29 to 296 years old (see Figure S8). The eucalypt cohort found in the TW rainforest site dated to 1859 (± 57 years) which may align with the 1851 fire. A eucalypt dating to the 1983 fire (29 years old ± 18 years) was found in the SK rainforest plot while the 1740 (± 68 years) and 1820 (± 65 years) cohorts in the eucalypt plot align with similar cohorts of *N. cunninghamii* in the SK rainforest plot. The oldest *N. cunninghamii* sampled (established pre-1700, Figure S5) were also found at this site suggesting a fire may also have occurred in the mid to late 1600s, this signal was also detected in at the DA eucalypt site that had *E. regnans* dating back to the mid-late 1600s (Fig S8). These fires suggest that the SK rainforest site likely burned in the late 1600s, the late 1700s, again in the 1820s, and again in 1983. Eucalypt cohorts in the DB rainforest plot was congruent with the DB eucalypt plot suggesting fires occurred around 1820 and in 1926. In the CV rainforest plot, eucalypt cohorts dated to 1719 (± 70 years) and 1944 (± 35 years). The 1787 and 1836 cohorts found in CV eucalypt plot align with similar cohorts of *N. cunninghamii* in the CV rainforest suggesting that a fires around 1730, in the 1770s-90s, in

1851, and again in 1939 burned this rainforest stand. Two eucalypt cohorts were identified at the DA rainforest site dating to 1803 (± 64 years) and 1913 (± 45 years). The 1803 cohort is consistent with the 1784 cohort identified in the DA eucalypt site while the 1851 signal in the rainforest trees (Fig S5) is consistent with the 1851 eucalypt cohort identified in the paired eucalypt site. The 1913 cohort could have come from the 1926 or 1939 fires though given the strong understorey signal for the 1926 fire in the eucalypt plot it is likely the former. These results suggest that at the DA rainforest site fires occurred in the 1650s-1680s, 1770s-90s, 1851, and 1926.

**References**

Ashton DH. 1976. The development of even-aged stands of *Eucalyptus regnans* F. Muell in Central Victoria. *Australian Journal of Botany* **24**: 397–414.

Benaglia T, Chauveau D, Hunter DR, Young D. 2009. mixtools: An R Package for Analyzing Finite Mixture Models. *Journal of Statistical Software* 32: 1–29.

Hunter DR, Wang S, Hettmansperger TP. 2007. Inference for Mixtures of Symmetric Distributions. *The Annals of Statistics* 35: 224–251.

Palmer JG, Cook ER, Turney CSM, Allen K, Fenwick P, Cook BI, O'Donnell A, Lough J, Grierson P, Baker P. 2015. Drought variability in the eastern Australia and New Zealand summer drought atlas (ANZDA, CE 1500–2012) modulated by the Interdecadal Pacific Oscillation. *Environmental Research Letters* 10: 124002.

R Core Team. 2016. R: A language and environment for statistical computing. R Foundation for Statistical Computing, Vienna, Austria. https://www.R-project.org/.

Sorensen RC. 1983. Teaching the characteristics of yield response with the Mitscherlich equation using computers. *Journal of Agronomic Education* 12: 21–25.

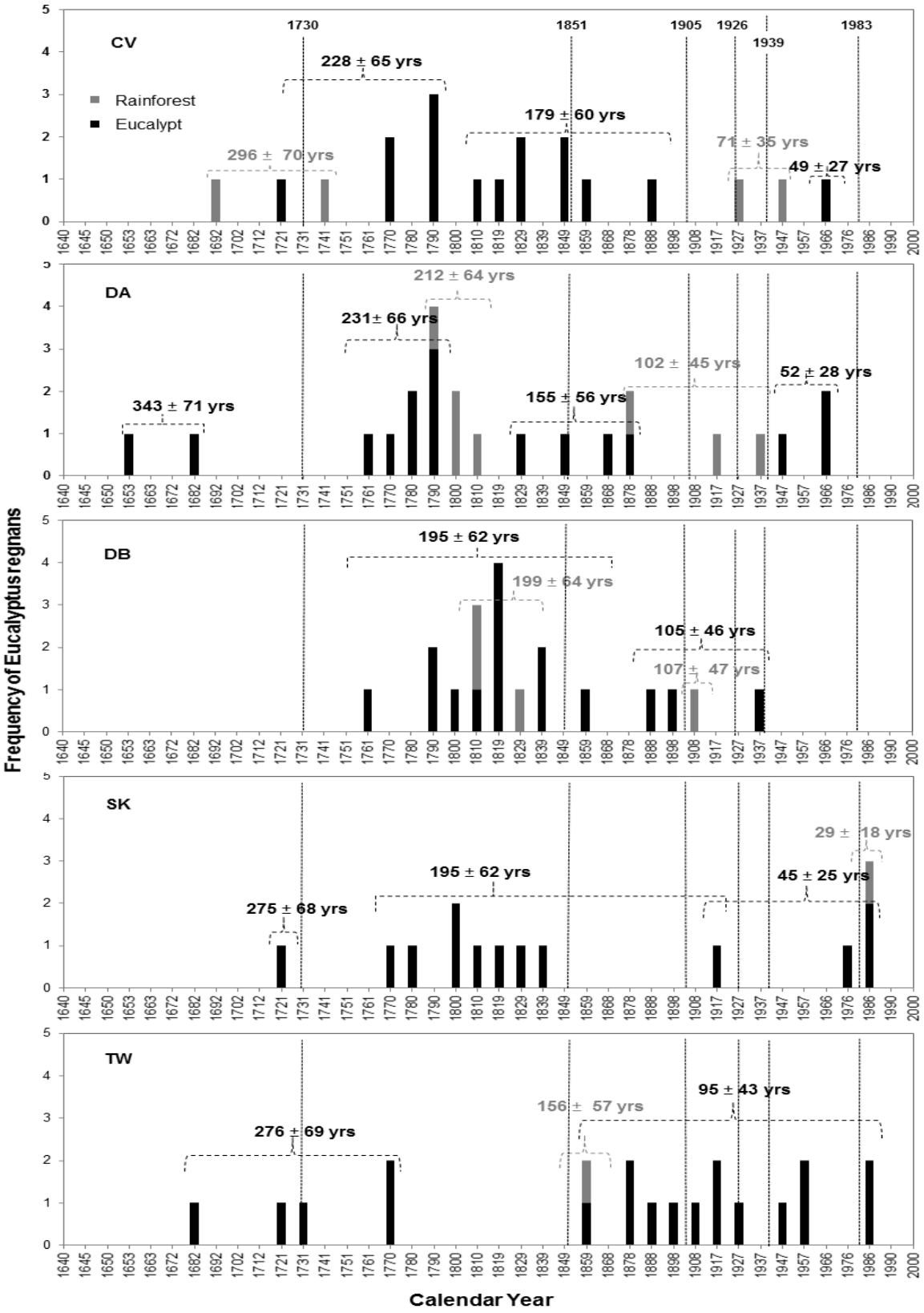


**Figure S8: Histogram of modelled tree ages for *Eucalyptus regnans* based on Ashton (1976) and estimated age cohorts (dashed brackets) based on mixture modelling for rainforest (grey) and old-growth (black) plots. Brackets indicate cohorts and associated values mean and 95% confidence intervals. Vertical dotted lines indicate known fire events in region, only 1939 and 1983 fires are mapped.**

**Appendix 8: Non-linear Relative Growth Rates of Blair et al. (2017) tree ferns**

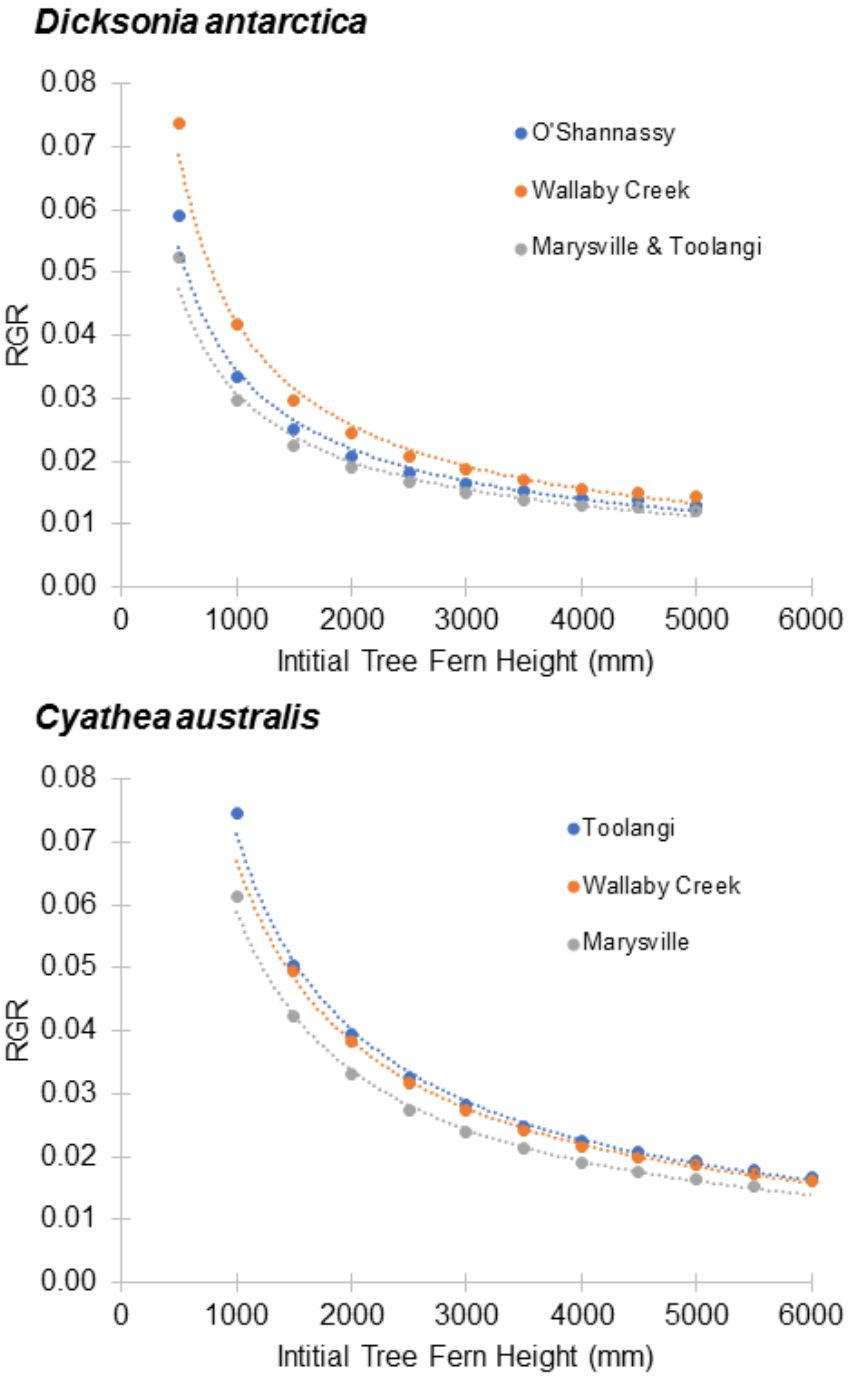


**Figure S9: Relative growth rates (RGR) of *Dicksonia antarctica* and *Cyathea australis* tree ferns approximated from Blair et al. (2017) from multiple sample locations. RGR are non-linear showing a decline in RGR with increasing initial tree fern size.**

## Reference

Blair DB, Blanchard W, Banks SC, Lindenmayer DB. 2017. Non-linear growth in tree ferns, *Dicksonia antarctica* and *Cyathea australis*. *PLoS ONE* 12: e0176908.